



# Free-convection boundary-layer flow of a non-Newtonian fluid along a vertical wavy surface

**M. Kumari**

Department of Mathematics, Indian Institute of Science, Bangalore, India

**I. Pop**

Faculty of Mathematics, University of Cluj, Cluj, Romania

**H. S. Takhar**

Manchester School of Engineering, University of Manchester, Manchester, UK

A theoretical analysis of laminar free-convection flow over a vertical isothermal wavy surface in a non-Newtonian power-law fluid is considered. The governing equations are first cast into a nondimensional form by using suitable boundary-layer variables that subtract out the effect of the wavy surface from the boundary conditions. The boundary-layer equations are then solved numerically by a very efficient implicit finite-difference method known as the Keller–Box method. A sinusoidal surface is used to elucidate the effects of the power-law index, amplitude wavelength, and Prandtl number on the velocity and temperature fields, as well as on the local Nusselt number. It is shown that the local Nusselt number varies periodically along the wavy surface. The wavelength of the local Nusselt number variation is half that of the wavy surface, irrespective of whether the fluid is a Newtonian fluid or a non-Newtonian fluid. Comparisons with earlier works are also made, and the agreement is found to be very good. © 1997 by Elsevier Science Inc.

**Keywords:** free convection; non-Newtonian fluids; power-law fluids; wavy surface

## Introduction

Interest in hydrodynamic and heat transfer problems of non-Newtonian fluids has grown considerably in recent years because of their wide use in chemicals, foods, polymers, molten plastics, sediments, petroleum production, and power engineering. Of general interest is the solution of the problem area of convective heat transfer between non-Newtonian fluids and two-dimensional (2-D) or axisymmetric bodies. Such a system has been analysed in the literature mainly for non-Newtonian power-law fluids emphasizing the effects of power-law index and generalised Prandtl number on the velocity and temperature fields, as well as on the skin friction and heat transfer coefficients. Acrivos (1960) was the first to study free-convection boundary-layer flow of a non-Newtonian power-law fluid along a vertical flat plate for large modified Prandtl numbers. Subsequently, a large amount of work (see for example, Reilly et al. 1965; Lee and Ames 1966; Na and Hansen 1966; Tien 1967; Sharma and Adelman 1969; Emery et al. 1970; Dale and Emery 1972; Chen and Wollersheim 1973;

Shulman et al. 1976; Kawase and Ulbrecht 1984; Som and Chen 1984; Wang and Kleinstreuer 1987; Haq et al. 1988; Huang et al. 1989; Huang and Chen 1990; Pop et al. 1991; Lee et al. 1992) including integral, experimental, and numerical methods to obtain solutions for a vertical flat plate with uniform wall temperature or uniform surface heat flux conditions. An account of most of the work carried out for non-Newtonian fluids before 1987 can be found in the review articles by Shenoy and Mashelkar (1982), Shenoy (1986), and Irvine and Karni (1987).

Studies of convective heat transfer in non-Newtonian fluids have focused mainly on flat plates and regular surfaces. However, there are, to the authors' knowledge, no studies on this problem for more complex geometries, such as wavy surfaces considered by Yao (1983), and Moulic and Yao (1989) for a Newtonian fluid, Chiu and Chou (1983, 1984) for a micropolar fluid, and Rees and Pop (1994, 1995) for fluid-saturated porous media.

In this paper, we study the effects of the longitudinal waves on the basic boundary-layer flow of a non-Newtonian power-law fluid induced by a uniformly heated vertical surface for which the resulting flow remains (2-D). The modified Grashof number is based on the wavelength of the longitudinal waves, and it is assumed to be large so that the boundary-layer approximation may be invoked. A transformation proposed by Yao (1983) was

---

Address reprint requests to Professor I. Pop at the Faculty of Mathematics, University of Cluj, R-3400 Cluj, CP253, Romania.

Received 26 May 1995; accepted 13 January 1997

Int. J. Heat and Fluid Flow 18: 625–631, 1997

© 1997 by Elsevier Science Inc.

655 Avenue of the Americas, New York, NY 10010

0142-727X/97/\$17.00  
PII S0142-727X(97)00024-6

used to transform a complex geometry into a simple shape. The advantage of this transformation is that the form of the boundary-layer equations remains invariant, and the surface conditions can, therefore, be applied on a transformed flat surface. Although the transformation itself is quite simple, it can handle very complex geometries. Thus, the flow described by a set of parabolic partial differential equations that is solved numerically using a very efficient finite-difference method, known as the Keller–Box method, described by Cebeci and Bradshaw (1984). A sinusoidal surface is used to investigate the effects of power law index, amplitude of the wavy surface, and generalised Prandtl number on the velocity and temperature profiles as well as on the local Nusselt number. The results obtained from this analysis are compared to those of Huang et al. (1989) for a flat plate and also to those of Chiu and Chou (1993) for the cases when there is a common overlap. In both cases, the results are found to be in very good agreement.

It should be mentioned that the prediction of heat transfer from irregular surfaces is a topic of fundamental importance. Irregularities in manufacturing frequently occur in practice. Surfaces are sometimes intentionally roughened to enhance heat transfer. Surfaces with intentionally placed roughness elements are encountered in several heat transfer devices. Some examples are flat-plate solar collectors and flat-plate condensers in refrigerators. The presence of roughness elements disturbs the flow past a flat surface and alters the heat transfer rate.

### Basic equations

The physical model considered is a vertical surface with transverse wavy surfaces at a constant temperature  $T_w$ , which is immersed in non-Newtonian power-law fluid of uniform ambient temperature  $T_\infty$ , where  $T_w > T_\infty$ . The geometry and coordinate system are illustrated in Figure 1. The wavy surfaces are described by

$$\bar{y} = \bar{\sigma}(\bar{x}) = \bar{a} \sin(k\bar{x}) \quad (1)$$

where  $\bar{a}$  is the amplitude of the wavy surface, and  $k$  is the wave number, given by  $k = 2\pi/L$ , with  $L$  being the characteristic length associated with the wavy surface. The governing equations

for a steady, laminar, and incompressible free-convection flow of a power-law fluid along a semi-infinite vertical surface of arbitrary shape can be written with Boussinesq approximation as (Bird et al. 1977),

$$\frac{\partial \bar{u}}{\partial \bar{x}} + \frac{\partial \bar{v}}{\partial \bar{y}} = 0 \quad (2)$$

$$\rho \left( \bar{u} \frac{\partial \bar{u}}{\partial \bar{x}} + \bar{v} \frac{\partial \bar{u}}{\partial \bar{y}} \right) = - \frac{\partial \bar{p}}{\partial \bar{x}} + \frac{\partial \bar{\tau}_{xx}}{\partial \bar{x}} + \frac{\partial \bar{\tau}_{xy}}{\partial \bar{y}} + \rho g \beta (T - T_\infty) \quad (3)$$

$$\rho \left( \bar{u} \frac{\partial \bar{v}}{\partial \bar{x}} + \bar{v} \frac{\partial \bar{v}}{\partial \bar{y}} \right) = - \frac{\partial \bar{p}}{\partial \bar{y}} + \frac{\partial \bar{\tau}_{yx}}{\partial \bar{x}} + \frac{\partial \bar{\tau}_{yy}}{\partial \bar{y}} \quad (4)$$

$$\bar{u} \frac{\partial T}{\partial \bar{x}} + \bar{v} \frac{\partial T}{\partial \bar{y}} = \alpha \left( \frac{\partial^2 T}{\partial \bar{x}^2} + \frac{\partial^2 T}{\partial \bar{y}^2} \right) \quad (5)$$

The stress tensor  $\bar{\tau}_{ij}$  is related to the rate of deformation tensor  $\bar{D}_{ij}$  by the relation

$$\bar{\tau}_{ij} = 2K \{2\bar{D}_{kl}\bar{D}_{kl}\}^{(n-1)/2} \cdot \bar{D}_{ij} \quad (6)$$

where  $\bar{D}_{ij}$  is defined as

$$\bar{D}_{ij} = \frac{1}{2} \left\{ \frac{\partial \bar{u}_i}{\partial \bar{x}_j} + \frac{\partial \bar{u}_j}{\partial \bar{x}_i} \right\} \quad (7)$$

The appropriate boundary conditions for Equations 2–5 are

$$\begin{aligned} \bar{y} = \bar{\sigma}(\bar{x}) : \bar{u} = \bar{v} = 0 \quad T = T_w \\ \bar{y} \rightarrow \infty : \bar{u} = \bar{v} = 0 \quad T = T_\infty \quad \bar{p} = \bar{p}_\infty \end{aligned} \quad (8)$$

### Notation

$a$	amplitude of longitudinal surface
$D_{ij}$	deformation tensor
$f$	reduced stream function
$g$	acceleration due to gravity
Gr	generalised Grashof number
$k$	wave number
$K$	consistency index
$L$	wavelength of the wavy surface
$n$	flow behaviour index
$\mathbf{N}$	unit vector normal to wavy surface
Nu	Local Nusselt number
$p$	pressure
Pr	generalised Prandtl number
$q$	heat flux
$T$	temperature
$\Delta T$	characteristic temperature
$u, v$	velocity components along $(x, y)$ -axes
$U_c$	characteristic velocity
$x$	axial (Cartesian) coordinate
$y$	transversal (Cartesian) coordinate

### Greek

$\alpha$	thermal diffusivity
$\beta$	thermal expansion coefficient
$\eta$	psuedosimilarity variable
$\theta$	dimensionless temperature
$\kappa$	thermal conductivity
$\rho$	density
$\sigma$	surface geometry function
$\tau_{ij}$	stress tensor
$\psi$	stream function

### Superscripts

$-$	dimensional variables
$/$	differentiation with respect to $\eta$

### Subscripts

$i, j, k, \ell$	indices
$x$	derivation with respect to $x$
$w$	wall condition
$\infty$	ambient condition

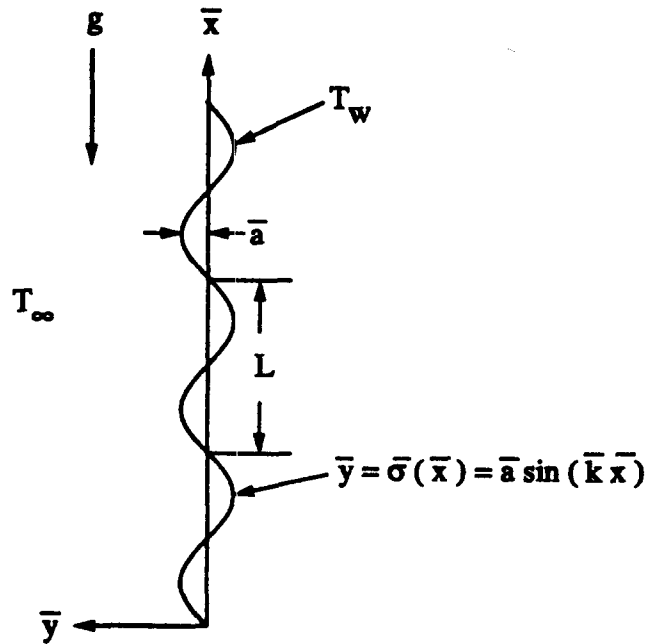


Figure 1 Physical model and coordinate system

Equations 2–5 may be transformed further by using suitable dimensionless variables, which subtract out the effect of the wavy surface from the boundary conditions (Equation 8), of the following form

$$\begin{aligned} x &= \bar{x}/L & y &= \frac{\bar{y} - \bar{\sigma}(\bar{x})}{L} \cdot Gr^{1/2(n+1)} & a &= \bar{a}/L \\ u &= \bar{u}/U_c & v &= \frac{\bar{v} - \sigma_x \bar{u}}{U_c} Gr^{1/2(n+1)} & p &= \bar{p}/\rho U_c^2 \\ \theta &= (T - T_\infty)/\Delta T & \sigma(x) &= \bar{\sigma}(\bar{x})/L & \sigma_x &= \frac{d\sigma}{dx} \\ \Delta T &= T_w - T_\infty & U_c &= (g\beta\Delta TL)^{1/2} \end{aligned} \quad (9)$$

where  $Gr = (g\beta\Delta T)^{2-n} L^{2+n} / (K/\rho)^2$  is the generalised Grashof number. Substituting Equation 9 into Equations 2–5 and formally lettering  $Gr \rightarrow \infty$  (boundary-layer approximation), then the leading order terms of the transformed equations become

$$\frac{\partial u}{\partial x} + \frac{\partial v}{\partial y} = 0 \quad (10)$$

$$\begin{aligned} u \frac{\partial u}{\partial x} + v \frac{\partial u}{\partial y} &= -\frac{\partial p}{\partial x} + \sigma_x Gr^{1/2(n+1)} \frac{\partial p}{\partial y} \\ &+ (1 + \sigma_x^2)^n \frac{\partial}{\partial y} \left[ \left| \frac{\partial u}{\partial y} \right|^{n-1} \frac{\partial u}{\partial y} \right] + \theta \end{aligned} \quad (11)$$

$$\begin{aligned} \sigma_{xx} u^2 + \sigma_x \left( u \frac{\partial u}{\partial x} + v \frac{\partial u}{\partial y} \right) \\ = -Gr^{1/2(n+1)} \frac{\partial p}{\partial y} + \sigma_x (1 + \sigma_x^2)^n \frac{\partial}{\partial y} \left[ \left| \frac{\partial u}{\partial y} \right|^{n-1} \frac{\partial u}{\partial y} \right] \end{aligned} \quad (12)$$

$$u \frac{\partial \theta}{\partial x} + v \frac{\partial \theta}{\partial y} = \frac{1 + \sigma_x^2}{Pr} \frac{\partial^2 \theta}{\partial y^2} \quad (13)$$

where  $Pr = (1/\alpha)(K/\rho)^{2/(1+n)} L^{(1-n)/(1+n)} U_c^{3(n-1)/2(n+1)}$  is the generalised Prandtl number.

Strictly speaking, this asymptotic analysis is valid only within the framework of boundary-layer scalings,  $y = 0$  ( $Gr^{-1/2(n+1)}$ ) and  $a = 0$  ( $Gr^{-1/2(n+1)}$ ) as  $Gr \rightarrow \infty$ , which resulted from Equation 9. Equation 12 indicates that  $(\partial p / \partial \bar{y})$  is  $O(Gr^{-1/2(n+1)})$ . This implies that the lowest-order pressure gradient along the  $x$ -direction is determined from the inviscid solution. However, for the present problem this gives  $(\partial p / \partial \bar{x}) = 0$ .

Next, to eliminate the term  $Gr^{1/2(n+1)} (\partial p / \partial \bar{y})$  from Equations 11 and 12, we multiply Equation 12 by  $\sigma_x$ , and the resulting equation is added to Equation 11. After a little algebra, we obtain the following transformed equation

$$\begin{aligned} u \frac{\partial u}{\partial x} + v \frac{\partial u}{\partial y} + \frac{\sigma_x \sigma_{xx}}{1 + \sigma_x^2} u^2 \\ = (1 + \sigma_x^2)^n \frac{\partial}{\partial y} \left[ \left| \frac{\partial u}{\partial y} \right|^{n-1} \frac{\partial u}{\partial y} \right] + \frac{\theta}{1 + \sigma_x^2} \end{aligned} \quad (14)$$

It is worth mentioning here that for  $n = 1$  (Newtonian fluid), Equations 13 and 14 reduce to those given by Yao (1983). The corresponding boundary conditions of Equations 10, 13, and 14 are now given by

$$\begin{aligned} y = 0: u = v = 0 \quad \theta = 1 \\ y \rightarrow \infty: u = 0 \quad \theta = 0 \end{aligned} \quad (15)$$

To reduce the equations to a form suitable for numerical solution, let us introduce the transformation

$$\begin{aligned} \psi &= (4x)^{(2n+1)/2(n+1)} f(x, \eta) & \theta &= \theta(x, \eta) \\ \eta &= y / (4x)^{n/2(n+1)} \end{aligned} \quad (16)$$

where  $\psi$  is the stream function defined in the usual way ( $u, v$ ) =  $(\partial \psi / \partial y, -\partial \psi / \partial x)$ . Equations 13 and 14 then become

$$\begin{aligned} (1 + \sigma_x^2)^n (|f'|^{n-1} f'')' + 2 \frac{2n+1}{n+1} f f'' - 2 \left( 1 + 2 \frac{\sigma_x \sigma_{xx}}{1 + \sigma_x^2} \right) (f')^2 \\ + \frac{\theta}{1 + \sigma_x^2} = (4x) \left( f' \frac{df'}{dx} - f'' \frac{\partial f}{\partial x} \right) \end{aligned} \quad (17)$$

$$\begin{aligned} \frac{1 + \sigma_x^2}{Pr} (4x)^{(1-n)2/(1+n)} \theta'' + 2 \frac{2n+1}{n+1} f \theta' \\ = (4x) \left( f' \frac{\partial \theta}{\partial x} - \theta' \frac{\partial f}{\partial x} \right) \end{aligned} \quad (18)$$

subject to the boundary conditions

$$\begin{aligned} \eta = 0: f = f' = 0 \quad \theta = 1 \\ \eta \rightarrow \infty: f' = 0 \quad \theta = 0 \end{aligned} \quad (19)$$

where primes denote differentiation with respect to  $\eta$ . We notice that if the present variables  $f$  and  $\eta$  are changed to  $(4)^{-(2n+1)/2(n+1)} f$  and  $(4)^{n/2(n+1)} \eta$ , Equations 17 and 18 reduce

**Table 1** Values of  $\{Nu/[Gr/(4x)^n]^{1/2(n+1)}\}$  for  $n=1$  (Newtonian fluid) and  $a=0$  (flat plate); variables are changed to  $(4)-(2n+1)/2(n+1)f$  and  $(4)/n/2(n+1)\eta$  for comparison

Pr	Huang et al. (1989)	Present results
10	0.8268	0.82609
100	1.5486	1.54739
1000	2.8084	2.80689

to those derived by Huang et al. (1989) for  $a=0$ ; i.e.,  $\sigma(x)=0$  (flat plate).

The physical quantity of interest in this problem is the local Nusselt number defined as

$$Nu = \frac{L\bar{q}_w}{\kappa\Delta T} \quad (20)$$

where the heat flux  $\bar{q}_w$  is given by

$$\bar{q}_w = -\kappa \mathbf{N} \cdot \nabla T \quad (21)$$

and the vector

$$\mathbf{N} = \left\{ -\frac{\sigma_x}{(1+\sigma_x^2)^{1/2}}, \frac{1}{(1+\sigma_x^2)^{1/2}} \right\} \quad (22)$$

is the unit vector normal to the wavy surface. Thus, we have

$$\bar{q}_w = -\kappa \left\{ -\frac{\sigma_x}{(1+\sigma_x^2)^{1/2}} \frac{\partial T}{\partial \bar{x}} + \frac{1}{(1+\sigma_x^2)^{1/2}} \frac{\partial T}{\partial \bar{y}} \right\}_{\bar{y}=\bar{\sigma}(\bar{x})} \quad (23)$$

or

$$\bar{q}_w = \frac{\kappa\Delta T}{L} \left\{ \frac{Gr}{(4x)^n} \right\}^{1/2(n+1)} (1+\sigma_x^2)^{1/2} [-\theta'(x,0)] \quad (24)$$

**Table 2** Values of  $\{Nu/[Gr/(4x)^n]^{1/2(n+1)}\}$  for  $n=1$  (Newtonian fluid) and  $Pr=1$ 

$x$	$a=0.1$		$a=0.2$	
	Chiu and Chou (1993)	Present	Chiu and Chou (1993)	Present
1.5	0.535919	0.53634	0.464354	0.48042
1.625	0.555911	0.53725	0.500265	0.48118
1.75	0.562036	0.54810	0.523690	0.50781
1.875	0.546929	0.54725	0.472925	0.50774
2.0	0.534797	0.53709	0.460098	0.48211
2.125	0.557163	0.53744	0.499669	0.48165
2.25	0.562414	0.54732	0.521798	0.50521
2.375	0.544776	0.54711	0.466142	0.50758
2.5	0.533628	0.53762	0.455783	0.48332
2.625	0.558064	0.53755	0.498469	0.48192
2.75	0.562696	0.54674	0.519818	0.50314
2.875	0.542824	0.54703	0.459938	0.50758
3.0	0.532453	0.53804	0.451472	0.48427

if Equations 9 and 16 are used. Therefore, the local Nusselt number defined by Equation 20 can be expressed as

$$Nu \left/ \left\{ \frac{Gr}{(4x)^n} \right\}^{1/2(n+1)} \right. = (1+\sigma_x^2)^{1/2} [-\theta'(x,0)] \quad (25)$$

## Results and discussion

Equations 17 and 18 subject to the boundary conditions (Equation 19) have been solved numerically using the Keller-Box method, which is described in the book by Cebeci and Bradshaw (1984). Representative results for the velocity and temperature profiles as well as for the local Nusselt number have been obtained for sinusoidal surfaces described by  $\sigma = a \sin(2\pi x)$  for amplitude wavelength  $a = 0.0$  (flat plate), 0.1 and 0.2. The flow index values are  $n = 0.5, 0.6, 0.8, 1.0$  (Newtonian fluid), 1.2 and 1.5, and the Prandtl number values are  $Pr = 6.7, 0.7, 1, 10, 100$ , and 1000. To verify the accuracy of the present method, the comparisons in the local Nusselt number given by Equation 25 have been shown in Table 1 for the case of a flat plate ( $a=0$ ) immersed in a Newtonian fluid ( $n=1$ ) with different Prandtl numbers. It is seen that the results of the present method are in excellent agreement with those of Huang et al. (1989).

We have also compared in Table 2 the present results for the local Nusselt number at different  $x$ -locations of the sinusoidal surface with those of Chiu and Chou (1993) obtained for a Newtonian fluid ( $n=1$ ). It is seen that the present results are in a favourable agreement with the results reported by Chiu and Chou (1993). The small difference may, however, be attributed to the different methods used. Chiu and Chou (1993) have used a

**Table 3** Values of  $\{Nu/[Gr/(4x)^n]^{1/2(n+1)}\}$  for  $x=1.75$  (trough)

Pr	$n$	$a=0$	$a=0.1$	$a=0.2$
0.7	0.6	0.43275	0.41585	0.38308
	0.8	0.46892	0.45131	0.41728
	1.0	0.49841	0.48001	0.44472
	1.2	0.52334	0.50400	0.46719
	1.5	0.55455	0.53400	0.49466
6.7	0.6	0.85471	0.81698	0.75918
	0.8	0.95291	0.91994	0.85526
	1.0	1.03974	1.00235	0.93035
	1.2	1.11245	1.07070	0.99101
	1.5	1.20304	1.15460	1.06423
10	0.6	0.93782	0.90578	0.84192
	0.8	1.06537	1.02746	0.95428
	1.0	1.16891	1.12514	1.04198
	1.2	1.25554	1.20568	1.11265
	1.5	1.36409	1.30562	1.19774
100	0.6	1.63168	1.54626	1.40583
	0.8	1.94976	1.83060	1.63961
	1.0	2.21251	2.06156	1.83045
	1.2	2.43543	2.25592	1.98836
	1.5	2.71709	2.50497	2.18638
1000	0.6	2.78835	2.52948	2.17619
	0.8	3.51516	3.17717	2.68315
	1.0	4.13570	3.75296	3.15439
	1.2	4.66234	4.24444	3.57471
	1.5	5.30515	4.84502	4.09476

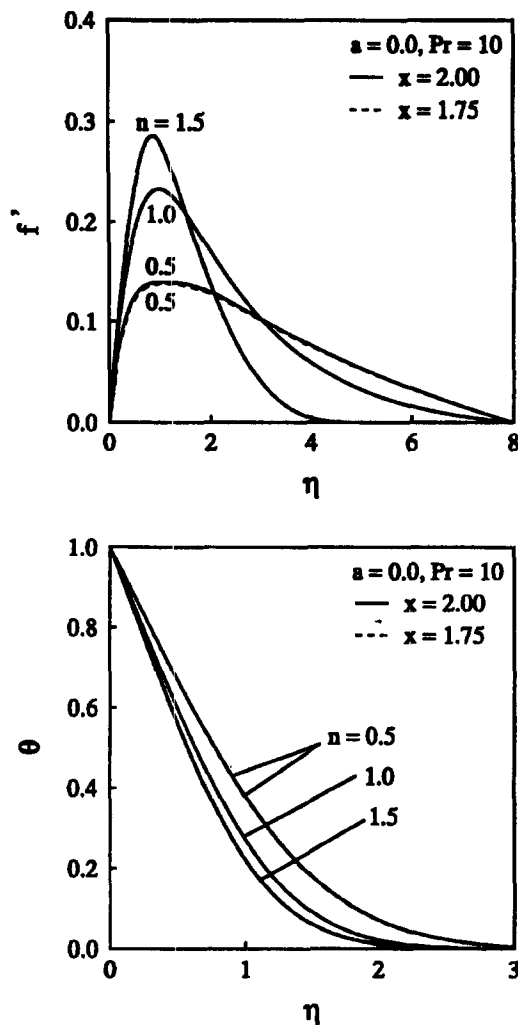


Figure 2 Dimensionless velocity and temperature profiles versus  $\eta$  for various flow behaviour index  $n$ :  $a=0$ ;  $x=1.75$ ; and  $2.0$ ,  $Pr=10$

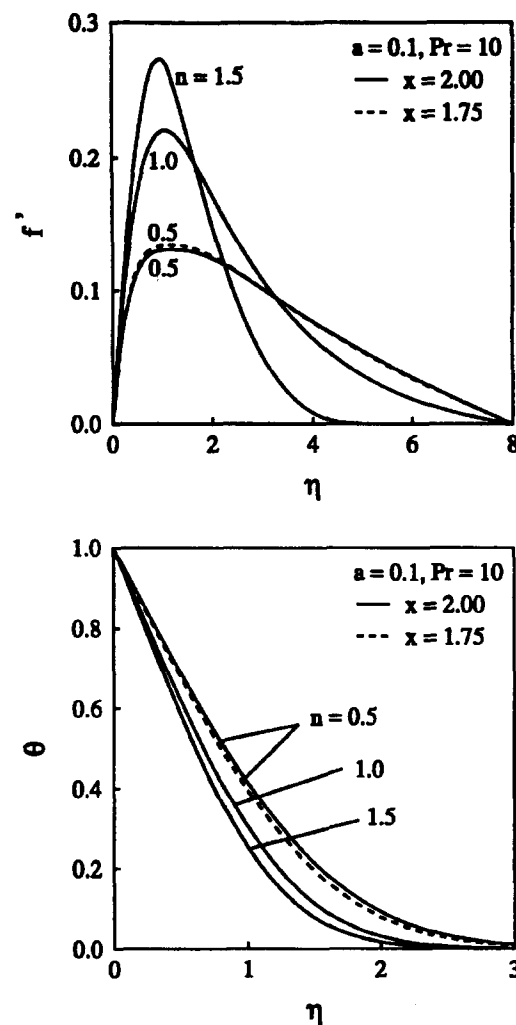


Figure 3 Dimensionless velocity and temperature profiles versus  $\eta$  for various flow behaviour index  $n$ :  $a=0.1$ ;  $x=1.75$ ; and  $2.0$ ,  $Pr=10$

cubic spline collocation method in combination with the finite-difference scheme, while we used the Keller box method.

The variation in the velocity  $f'$  and temperature  $\theta$  profiles with the power-law index  $n$  and amplitude wavelength  $a$  are presented in Figures 2 to 5 for  $Pr=10$ . However, it should be mentioned that the behaviour between these profiles at  $x=1.5$  (node) and  $x=2.0$  (node) is similar in this study, as is the case between the profiles at  $x=1.75$  (trough) and  $x=2.25$  (crest). For convenience, therefore, cases  $x=1.75$  and  $x=2.0$  only are described here. It is seen from Figure 2, as expected, that for a flat plate ( $a=0$ ) the hydrodynamic boundary-layer thicknesses are almost equal at the two positions considered. The same is true also for the thermal boundary layer. However, the velocity profiles increase, while the temperature profiles decrease with the increase of  $n$ . Furthermore, Figures 3 and 4 show that for a wavy surface ( $a \neq 0$ ) the hydrodynamic boundary-layer thickness grows near the trough position, but only for  $n < 1$  (pseudoplastic fluids). However, the thermal boundary layer decreases at  $x=1.75$  (trough). The local Nusselt number defined by Equation 25 is shown in Table 3 for  $x=1.75$  and some values of  $a$ ,  $n$ , and  $Pr$ .

The variation of the local Nusselt number versus  $x$  is also shown in Figures 5–7 for  $a=0$  (flat plate),  $0.1$ , and  $0.2$  and some values of  $n$  when  $Pr=10$ . It is observed that the local Nusselt number increases as  $n$  increases. The wavy variation of the local

Nusselt number can be observed only near the leading edge and gradually disappears downstream where the boundary layer grows thick. These figures also show that the wavelength of the local Nusselt number is only half that of the wavy surface. This is because of (1) the effect of centrifugal forces, the third term of Equation 17; and (2) the alignment of the buoyancy force with respect to the solid surface, as indicated by the fourth term of Equation 17. For the wavy surface, the important component of the buoyancy force (that component tangential to the wavy surface) is less than the total buoyancy force, except at the crests and troughs of the wave surface. Consequently, at any  $x$ -location, the thermal boundary layer for the flat plate ( $a=0$ ) is thinner than that for the wavy surface (see Table 3), because the buoyancy force that accelerates the fluid near the wall is larger. It is also seen in Table 3 that the local Nusselt number increases with both  $n$  and  $Pr$ . However, the Newtonian fluid ( $n=1$ ) is found to have a higher local heat transfer rates than pseudoplastic fluids ( $n < 1$ ) and lower values than dilatant fluids ( $n > 1$ ) (see also Huang et al. 1989). Furthermore, we note from Figures 5–7 that, at the leading edge of the wavy wall ( $x \rightarrow 0$ ), the local Nusselt number decreases for  $n < 1$  (pseudoplastic fluids) and increases for  $n > 1$  (dilatant fluids). This may be explained mathematically as follows. For  $x \rightarrow 0$ , the coefficient of the highest derivative in the energy Equation 18 is dominant for  $n > 1$  and very small for

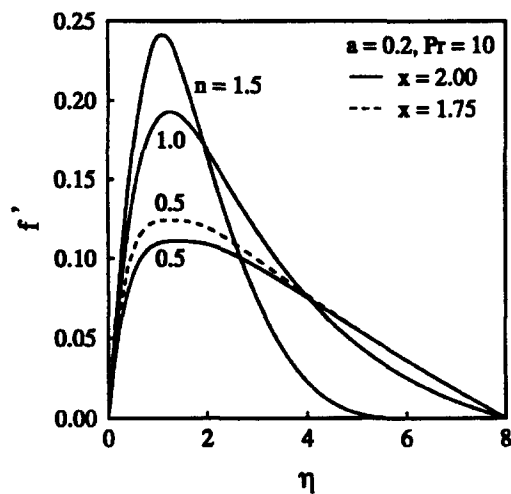


Figure 4 Dimensionless velocity and temperature profiles versus  $\eta$  for various flow behaviour index  $n$ :  $a=0.2$ ;  $x=1.75$ ; and  $2.0$ ,  $Pr=10$

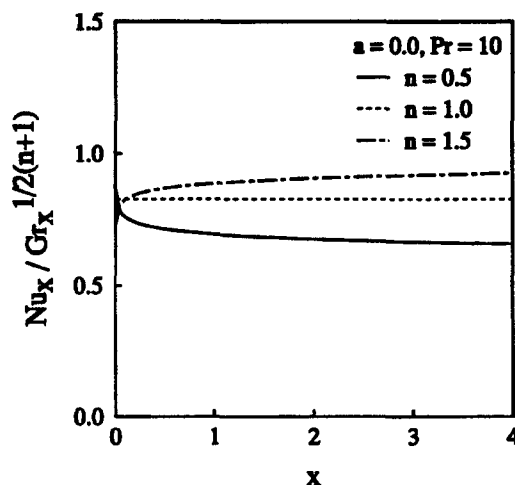


Figure 5 Variation of the local Nusselt number versus  $x$  for various flow behaviour index  $n$ :  $a=0$  (flat plate);  $Pr=10$

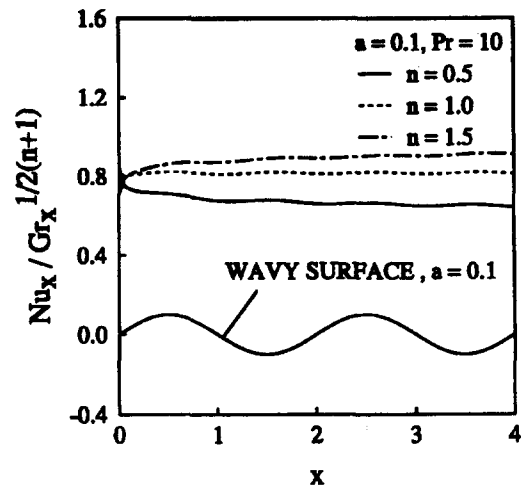


Figure 6 Variation of the local Nusselt number versus  $x$  for various flow behaviour index  $n$ :  $a=0.1$ ;  $Pr=10$

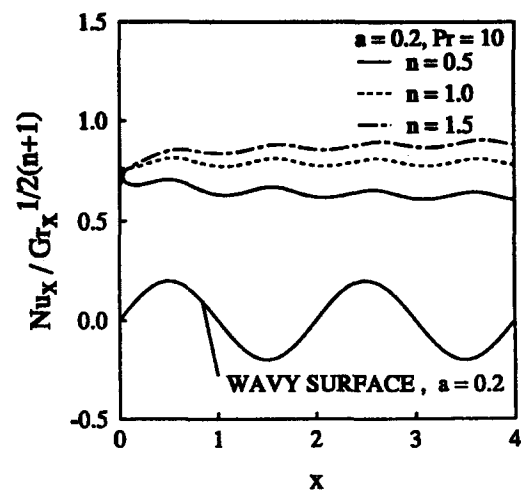


Figure 7 Variation of the local Nusselt number versus  $x$  for various flow behaviour index  $n$ :  $a=0.2$ ;  $Pr=10$

$n < 1$ . This, therefore, implies that the magnitude of the local Nusselt number near the leading edge is very high for pseudoplastic fluids and low for dilatant fluids. As  $x$  increases, the difference reduces quickly, and at certain  $x$ -values, the local Nusselt number for dilatant fluids exceed those for pseudoplastics. This is in agreement with the results of Huang et al. (1989). It is hoped that experimental data will become available in the near future to verify the results of the present investigation.

### Acknowledgments

We very much appreciate the constructive suggestions made by the reviewers of the original manuscript.

### References

- Acrivos, A. 1960. A theoretical analysis of laminar natural convection heat transfer to non-Newtonian fluids. *AIChE J.*, **16**, 584-590
- Bird, R. B., Armstrong, R. C. and Hassager, O. 1977. *Dynamics of Polymeric Liquids*, Vol. 1, Fluid Mechanics, Wiley, New York

- Cebeci, T. and Bradshaw, P. 1984 *Physical and Computational Aspects of Convective Heat Transfer*, Springer, New York, 406–415
- Chen, T. V. W. and Wollersheim, D. E. 1973. Free convection at a vertical plate with uniform flux condition in non-Newtonian power-law fluids. *J. Heat Transfer* **95**, 123–124
- Chiu, C. P. and Chow, H. M. 1993. Free convection in the boundary-layer flow of a micropolar fluid along a vertical wavy surface. *Acta Mechanica*, **101**, 161–174
- Chiu, C. P. and Chou, H. M. 1994. Transient analysis of natural convection along a vertical wavy surface in micropolar fluids. *Int. J. Eng. Sci.* **32**, 19–33
- Dale, J. D. and Emery, A. F. 1972. The free convection of heat from a vertical plate to several non-Newtonian pseudoplastic fluids. *J. Heat Transfer* **94**, 64–72
- Emery, A. F., Chi, H. S. and Dale, J. D. 1970. Free-convection through vertical plane layers of non-Newtonian power-law fluids. *J. Heat Transfer*, **93**, 164–171
- Haq, S., Kleinstreuer, C. and Mulligan, J. C. 1988. Transient free convection of a non-Newtonian fluid along a vertical wall. *J. Heat Transfer*, **110**, 604–607
- Huang, M. J., Huang, J. S., Chou, Y. L. and Chen, C. K. 1989. Effects of Prandtl number on free-convection heat transfer from a vertical plate to a non-Newtonian fluid. *J. Heat Transfer* **111**, 189–191
- Huang, M. J. and Chen, C. K. 1990. Local similarity solutions of free-convective heat transfer from a vertical plate to non-Newtonian power-law fluids. *Int. J. Heat Mass Transfer*, **33**, 119–125
- Irvine, T. F. and Karni, J. 1987. Non-Newtonian fluid flow and heat transfer. In: *Handbook of Single-Phase Convective Heat Transfer*, S. Kakac, R. K. Shah and W. Aung (eds.) Wiley, New York, 20.1–20.57
- Kawase, K. and Ulbrecht, J. 1984. Approximate solution to the natural convection heat transfer from a vertical plate. *Int. Comm. Heat Mass Transfer* **11**, 143–155
- Lee, J. K., Gorla, R. S. R. and Pop, I. 1992. Natural convection to power-law fluids from a heated vertical plate in a stratified environment. *Int. J. Heat Fluid Flow*, **12**, 259–265
- Lee, S. Y. and Ames, W. F. 1966. Similarity solutions for non-Newtonian fluids. *AIChE J.*, **22**, 700–708
- Moulic, S. G. and Yao, L. S. 1989. Natural convection along a vertical wavy surface with uniform heat flux. *J. Heat Transfer*, **111**, 1106–1108
- Na, T. Y. and Hansen, A. G. 1966. Possible similarity solutions of the laminar natural convection flow of non-Newtonian fluids. *Int. J. Heat Mass Transfer* **9**, 261–262
- Pop, I., Rashidi, M. and Gorla, R. S. R. 1991. Mixed convection to power-law type non-Newtonian fluids from a vertical wall. *Polymer-Plastics Tech. Eng.* **30**, 47–66
- Rees, D. A. S. and Pop, I. 1994. A note on free convection along a vertical wavy surface in a porous medium. *J. Heat Transfer* **116**, 505–508
- Rees, D. A. S. and Pop, I. 1995. Free convection induced by a vertical wavy surface with uniform heat flux in a porous medium. *J. Heat Transfer* **117**, 547–550
- Reilly, I. G., Tien, C. and Adelman, M. 1965. Experimental study of natural convection heat transfer from a vertical plate in non-Newtonian fluids. *Can. J. Chem. Eng.* **43**, 157–160
- Sharma, K. K. and Adelman, M. 1969. Experimental study of natural convection heat transfer from a vertical plate in a non-Newtonian fluid. *Can. J. Chem. Eng.* **47**, 553–555
- Shenoy, A. V. and Mashelkar, R. A. 1982. Thermal convection in non-Newtonian fluids. In *Advances in Heat Transfer*, Vol. 15, Academic Press, New York, 143–225
- Shenoy, A. V. 1986. Natural convection heat transfer to power-law fluids. In *Handbook of Heat and Mass Transfer*, N. P. Chermisnoff (ed.), Gulf Publishing, Houston, Texas, USA, 183–210
- Shulman, Z. P., Baikov, V. I. and Zaltsgendler, E. A. 1976. An approach to prediction of free convection in non-Newtonian fluids. *Int. J. Heat Mass Transfer*, **19**, 1003–1007
- Som, A. and Chen, J. L. S. 1984. Free convection of non-Newtonian fluids over nonisothermal two-dimensional bodies. *Int. J. Heat Mass Transfer*, **27**, 791–794
- Tien, C. 1967. Laminar natural convection heat transfer to non-Newtonian fluids. *Appl. Sci. Res.*, **17**, 233–248
- Wang, T. Y. and Kleinstreuer, C. 1987. Free-convection heat transfer between a permeable vertical wall and a power-law fluid. *Numer. Heat Transfer*, **12**, 367–379
- Yao, L. S. 1983. Natural convection along a vertical wavy surface. *J. Heat Transfer*, **105**, 465–468